

Bakuchiol protects against adverse cardiac remodeling after myocardial infarction

Yun-Jiao Duan[#], Zhu-Xia Shen[#], Ting Huang, Hui-Hui Gu, Yu-Tian Wu, Yu-Min Sun, Jun Wang*

Abstract

Background: Myocardial infarction (MI) is closely related to heart failure and death. Cardiac fibrosis after MI is related to profound changes in cardiac structure and geometry, leading to decreased cardiac function. Unfortunately, effective therapies to prevent excessive cardiac fibrosis and improve cardiac function are limited. Consequently, new therapeutic strategies are urgently required to protect cardiac function after MI. Bakuchiol (BAK), extracted from the plant seeds of *Psoralea corylifolia*, has shown protective effects against pathological cardiac hypertrophy. However, it is unclear whether BAK could improve cardiac function and reduce cardiac fibrosis after MI.

Objective: To assess the reportability of bakuchiol as an alternative treatment against adverse cardiac remodeling after myocardial infarction.

Methods: To address this question, a MI model was built on adult wild-type C57/BL 6N mice (male, 6–8 weeks, Zhejiang Vital River Laboratory Animal Technology Co., Ltd) by left coronary artery ligation and gavage with BAK (60 mg/kg/day) for 28 consecutive days. Chest cardiac ultrasonography was performed 7 and 28 days after MI using the Vevo 2100 system to assess ventricular shape and function in model mice. The effects of BAK on cardiac remodeling and function were assessed after MI. Effects of BAK on isoprenaline-induced cardiac fibroblast proliferation and migration were also studied.

Results: After MI injury, BAK can attenuate adverse cardiac remodeling and maintain left ventricular ejection fraction and fraction shortening. Furthermore, mice treated with BAK after MI injury showed lower fibrosis and wider left ventricular thickness than those without BAK. In addition, BAK can inhibit cardiac myofibroblast differentiation after MI. After stimulation with isoprenaline, BAK inhibited cardiac fibroblast proliferation and migration. At the molecular level, extracellular signal-regulated kinase 2 (ERK2) and transforming growth factor (TGF)- β 1 were inhibited in both MI mice and isoprenaline-stimulated cardiac fibroblasts after BAK treatment.

Conclusions: Our data suggest that BAK treatment, as a novel therapeutic strategy, protects against adverse cardiac remodeling and maintains cardiac function after MI, likely via the ERK2 and TGF- β 1 signaling pathways.

[*Ethiop. J. Health Dev.* 2021; 35(3):208-219]

Key Words : Bakuchiol, myocardial infarction, cardiac fibrosis, cardiac fibroblast, ERK2, TGF- β 1

Introduction

Myocardial infarction (MI) is closely related to morbidity of heart failure and death globally. Most myocardial tissue is not regenerative, and a stable scar rapidly forms to prevent cardiac rupture after acute MI (1). In the face of MI injury, cardiac remodeling is an essential pathological alteration to maintain cardiac compensation (2,3). However, the severity of cardiac fibrosis during cardiac remodeling is associated with cardiac dysfunction and the progressive development

of heart failure (4).

Cardiac fibroblasts are responsible for cardiac fibrosis after MI injury (5,6). After MI injury, the fibroblasts in the non-infarcted zone migrate and replace the necrotic cardiomyocytes in the infarcted area (7,8). In response to multiple stimuli, such as chemical and mechanical signals (5), the cardiac fibroblast proliferates and differentiates between compensating for cardiac function and maintaining normal cardiac remodeling (4). The myofibroblast differentiation would reach its

peak at 7-10 days post-myocardial infarction (8). However, excessive migration, proliferation, and differentiation of the fibroblast can increase the level of cardiac fibrosis and damage cardiac remodeling (7,8). Therefore, inhibition of the fibroblast in the infarcted zone may improve cardiac remodeling and function after MI (3). However, effective antifibrotic therapies after MI are currently limited (4).

Psoralea corylifolia (Leguminosae) has been used in traditional Chinese medicine and Ayurvedic medicine (9). Bakuchiol (BAK) is isolated from *Psoralea corylifolia* (10). BAK has anti-inflammatory (10,11), anti-aging (12), antioxidative (13), and anti-hyperglycemic (9) properties. Meanwhile, BAK has protective effects on the liver (14), lungs (15) and retina (16). However, only a few studies have investigated its effect on the heart, such as these below. The cardioprotective effect of BAK has been found to attenuate ischemia-reperfusion, injury-induced mitochondrial oxidative damage in isolated hearts (17), improve aortic banding-induced pathological cardiac hypertrophy (18), and reduce antioxidative effects in hyperglycemia-induced diabetic cardiomyopathy (19). However, the effects of BAK in regulating cardiac function and fibrosis after MI remain unclear. This research aimed to explore whether BAK improves cardiac function and attenuates fibrosis after MI, as well as to explore the underlying mechanisms of these attributes.

Materials and Methods

Animals and MI model:

Adult wild-type C57/BL 6N mice (male, 6–8 weeks, Zhejiang Vital River Laboratory Animal Technology Co., Ltd) were randomly divided into the following four groups (20): (i) sham group; (ii) sham+BAK

group (60 mg/kg/day); (iii) MI group; and (iv) MI+BAK group (60 mg/kg/day), according to the previous study (19, 21).

Mice in the MI/MI+BAK group had a permanent ligation operation on the left coronary artery to build a MI model. Mice in the sham/sham+BAK group underwent surgery to open the chest without ligation. All animal protocols in this research were approved by the Animal Care and Use Committee of Fudan University, following the National Institutes of Health guidelines or the care and use of laboratory animals.

After surgery, the mice in BAK groups were administered with BAK ($\geq 98\%$, Shanghai Winherb Medical Technology) and were suspended in 0.5% carboxymethylcellulose solution for 28 consecutive days, whereas the mice in the sham/MI group were administered with 0.5% carboxymethylcellulose solution at the same intervals (17, 18, 22).

Echocardiography

Trans-Thoracic Echocardiography (TTE) is the most widely known type of core ultrasonography for still images and recordings of the inner part of the heart using ultrasound. The chest or intermediate area in question is examined using the ultrasound transducer to get unique heart signs. It is used for non-interfering assessment of the heart's overall health, including the heart valves and heart muscles (an indicator of the rate of craving). Photos are displayed and recorded on the screen for continuous presentations. Transthoracic echocardiography was performed to assess ventricular geometry and function of model mice at 7- and 28-days post MI using the Vevo 2100 system. The related parameters were shown in fig.1 and table 1 and 2.

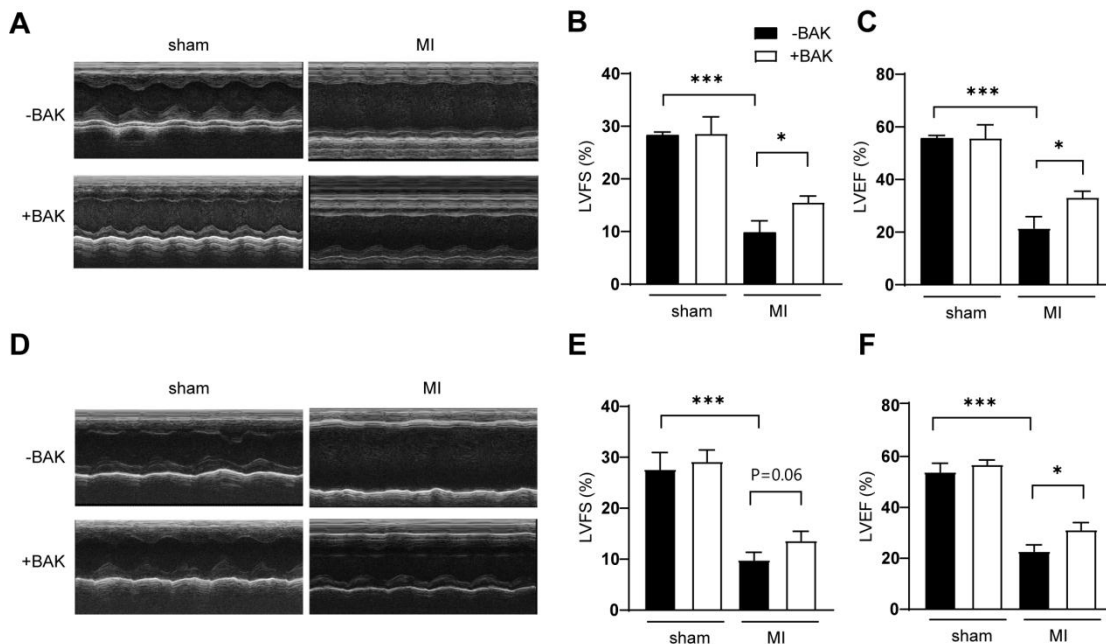


Fig.1. BAK improved cardiac function after MI injury. A. Representative echocardiographic images at 7 days post MI. B. Left ventricular fraction shortening (LVFS) at 7 days. C. Left ventricular ejection fraction (LVEF) at 7 days. D. Representative echocardiographic images at 28 days post MI. E. LVFS at 28 days. F. LVEF at 28 days. (sham/sham+BAK group: n=3-8, MI/MI+BAK group: n=6-9). *P<0.05, ***P<0.001.

Table 1. Echocardiographic parameters of cardiac function in BAK-treated MI mice on the 7th day.

	Sham	Sham+BAK	MI	MI+BAK
HR (beats/min)	411±52.40	408±39.31	368±51.53	406±61.86
LVEF (%)	55.71±2.75	55.64±8.91	21.54±9.83 ^{****}	33.11±6.34 [#]
LVFS (%)	28.34±1.55	28.56±5.59	9.86±4.9 ^{****}	15.50±3.17 [#]
IVSd (mm)	0.67±0.04	0.62±0.03	0.39±0.09 ^{****}	0.47±0.18
IVSs (mm)	1.10±0.06	0.91±0.07 ^{**}	0.54±0.08 ^{****}	0.62±0.22
LVEDV (μL)	54.32±16.22	52.22±9.94	78.38±19.15 [*]	67.47±18.32
LVESV (uL)	24.39±8.15	23.95±9.12	62.13±18.92 ^{***}	45.76±14.38
LVIDd (mm)	3.56±0.47	3.52±0.18	4.17±0.42 [*]	3.93±0.46
LVIDs (mm)	2.55±0.37	2.53±0.39	3.77±0.48 ^{***}	3.36±0.46
LVPWd (mm)	0.64±0.12	0.63±0.08	0.57±0.27	0.51±0.13
LVPWs (mm)	0.98±0.11	0.99±0.12	0.71±0.34	0.71±0.16

HR: heart rate, IVSd: end-diastolic interventricular septal thickness, IVSs: end-systolic interventricular septal thickness, LVEDV: left ventricular end-diastolic volume, LVESV: left ventricular end-systolic volume, LVIDd/s: left ventricular internal diameter at diastole/systole, LVPWd/s: left ventricular posterior wall thickness at end diastole/systole. *P<0.05, **P<0.01, ***P<0.001, ****P<0.0001 vs sham group. #P<0.05 vs MI group.

Table 2. Echocardiographic parameters of cardiac function in BAK-treated MI mice on the 28th day.

	Sham	Sham+BAK	MI	MI+BAK
HR (beats/min)	391.94±82.19	403.37±15.23	366.70±31.41	386.59±75.93
LVEF (%)	53.87±10.43	56.82±3.12	22.79±7.76 ^{****}	31.25±10.64 [#]
LVFS (%)	27.65±6.62	29.19±2.25	9.85±3.65 ^{***}	13.66±5.49
IVSd (mm)	0.66±0.11	0.67±0.02	0.46±0.15 [*]	0.43±0.13
IVSs (mm)	1.08±0.20	1.08±0.16	0.57±0.18 ^{***}	0.57±0.22
LVEDV (ul)	58.35±14.59	57.76±10.26	109.03±53.48 [*]	75.46±21.78
LVESV (ul)	26.41±6.34	24.64±2.63	89.07±52.00 ^{***}	54.90±21.49 ^{##}
LVIDd (mm)	3.68±0.36	3.68±0.28	4.70±0.98 [*]	4.09±0.50
LVIDs (mm)	2.66±0.27	2.60±0.11	4.27±1.05 ^{**}	3.55±0.60
LVPWd (mm)	0.67±0.06	0.64±0.05	0.41±0.13 ^{**}	0.44±0.09
LVPWs (mm)	0.97±0.12	1.08±0.04	0.54±0.23 ^{**}	0.59±0.12

*P<0.05, **P<0.01, ***P<0.001, ****P<0.0001 vs sham group.

#P<0.05, ##P<0.01 vs MI group.

Histological analysis

The isolated hearts were fixed in 4% PFA and then embedded into wax blocks for sectioning. Each heart slice was parallel to the short axis and stained with HE and Masson's trichrome. The heart slides were photographed and analyzed using an Olympus light microscope. Fibrosis, defined as blue collagen staining in Masson's trichrome, also represented the scar zone (23). The percentage of left ventricular fibrosis and ventricular thickness was calculated using Image J V1.8.0 (24).

The slides were stained with primary antibodies overnight for immunofluorescence staining and then stained with secondary antibodies. In addition, the

slides were counterstained with DAPI. The antibodies were as follows: anti- α -SMA (1:100, Service) and anti-Vimentin (1:100, Affinity).

Polymerase chain reaction analysis of gene expression

Total RNA was extracted using a cell/tissue RNA-quick purification kit (ES Science). The quantitative real-time PCR (qPCR) assay was performed using the LightCycler® 480 (Roche, Switzerland). All qPCR samples were run in triplicate, and the data was averaged. Sequences of the qPCR primer used in this study have been presented in Table 3.

Table 3. Sequences of the qPCR primers.

	Forward Primer	Reverse Primer
GAPDH	ATGTTCCAGTATGACTCCACTCACG	GAAGACACCAGTAGACTCCACGACA
TGF- β 1	CTTGCCCTCTACAACCAACA	ACTTGCGACCCACGTAGTAGA
ERK1	TCCGCCATGAGAATGTTATAGGC	GGTGGTGTGATAAGCAGATTGG
ERK2	CAGGTGTTTCGACGTAGGGC	TCTGGTGCTCAAAAGGACTGA
fibronectin	GAAGGTTTGCAACCCACTGT	TCTGCAGTGTCTCTTACC
α -SMA	GGCTCTGGGCTCTGTAAGG	CTCTTGCTCTGGGCTTCATC
α -MHC	TGCACTACGGAAACATGAAGTT	CGATGGAATAGTACACTTGCTGT
β -MHC	ACTGTCAACACTAAGAGGGTCA	TTGGATGATTTGATCTTCCAGGG
ANP	GCTTCCAGGCCATATTGGAG	GGGGCATGACCTCATCTT
BNP	ATGGATCTCCTGAAGGTGCTG	GTGCTGCCTTGAGACCGAA

Primary cardiac fibroblast culture

The cardiac fibroblasts were isolated from C57BL/6N mice for primary culture (25). Ventricles were removed and digested with 0.1% collagenase II. The fibroblasts were cultured in a medium (DME/F12, 10% FBS, 37 °C, 5% CO₂). The fibroblasts were used after the third passage. Fibroblasts were cultured in serum-free DME/F12 for 24 h, and then stimulated with or without isoprenaline (ISO, 20 µM, Sigma), with or without BAK, for 24 h (26, 27).

Cell proliferation assay

The cardiac fibroblasts were incubated in 96-well plates in 200 µL serum-free DME/F12 for 24 h and set in the presence or absence of BAK (0, 1, 2.5, 5 µM), with/without 20 µM ISO, for 24 h. The supernatant was then replaced with DME/F12 and Cell Counting Kit-8 (CCK8, Beyotime) in each well. Two hours later, OD values were measured at 450 nm.

Cell migration analysis

Transwell assays were used to evaluate the cardiac fibroblast migration rate. First, the fibroblasts (2×10^4 , 200 µL serum-free DME/F12) were added to the upper chamber of a 24-well cell culture chamber (BD falcon, 353097). Then, the lower section was added with 500 µL 10% FBS DME/F12 in different stimulation treatments as mentioned in the cell proliferation assay. After 24 h, the fibroblasts were fixed with 4% PFA and stained by crystal violet (25). After staining, five high-power fields ($\times 200$) were counted to analyze the average number of migrated cardiac fibroblasts per field by image J V1.8.0.

Statistical analysis

Data was analyzed for significance using an unpaired *t*-test via GraphPad Prism 8.0 software. All data was reported as mean \pm SEM. The difference was considered to be statistically significant with P values less than 0.05.

Results**BAK improved the cardiac function after MI**

Echocardiography was used at 7 and 28 days post-MI to assess contractile function. The MI mice exhibited a trend towards decreasing systolic dysfunction and increased dilative remodeling. Cardiac systolic function was evaluated by LVFS and LVEF, compared with the MI group, both parameters at 7 and 28 days showed noticeable improvement in the MI+BAK group (Fig.1). As shown in Tables 1 and 2, LVESV showed a decreasing trend at 7 and 28 days, compared with the MI group, LVESV had significantly improved in the MI+BAK group. LVIDd, LVIDs, and LVEDV, the MI+BAK group, showed a decreasing trend compared with the MI group. In cardiac structure, LVPWs, LVPWd, IVSd, and IVSs in the MI and MI+BAK groups had no significant differences. As a result, BAK treatment protected cardiac function after MI.

Effects of BAK on the cardiac structure after MI

After confirming the improvement of cardiac function for BAK treatment, HE staining, and Masson staining was conducted to evaluate the effect of BAK on the cardiac structure at 7 and 28 days post-MI (Fig.2). Changes in left ventricular fibrosis, wall thickness, and cross-sectional area (CSA) of cardiomyocytes in a remote location were detected.

Left ventricular fibrosis and wall thickness was evaluated by Masson staining (Fig.2A–C). Compared to the sham group, the level of fibrosis significantly increased in the MI group at 7 days, but compared with the MI group, BAK treatment significantly reduced fibrosis in the left ventricle in the MI+BAK group (Fig.2B). The left ventricular wall thickness decreased considerably in the MI group as compared to the sham group at 7 days, but BAK treatment recovered the decrease significantly at 7 and 28 days (Fig.2C). In remote areas, the cardiomyocyte CSA in the MI group was significantly greater than that in the sham group. After BAK treatment, the CSA of cardiomyocytes had no significant differences at 7 and 28 days (Fig.2D, E). Taken together, BAK treatments improved the cardiac tissue structure in a MI model.

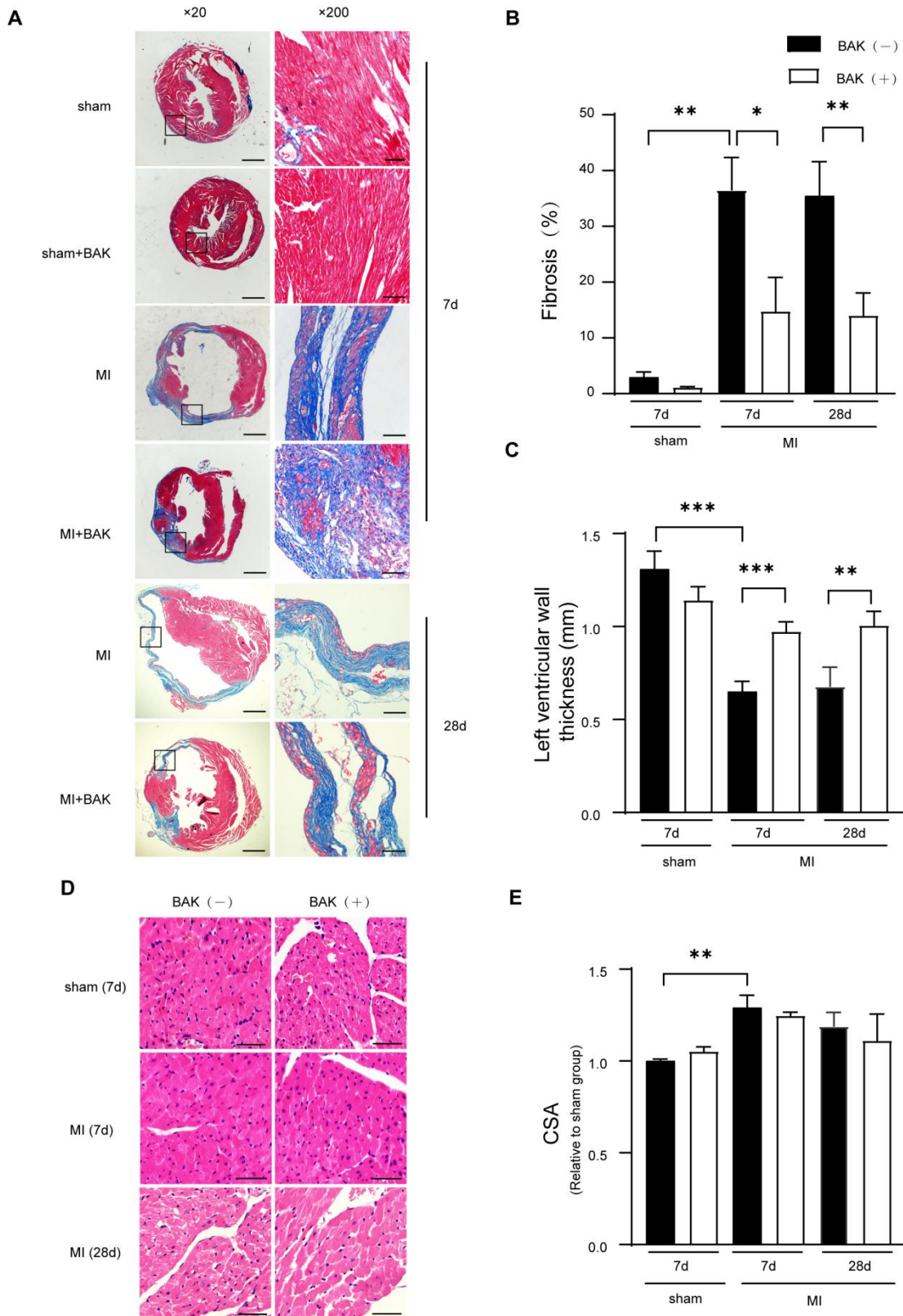


Fig.2. BAK improved cardiac structure after MI. A. Effect of BAK on the cardiac structure in the left ventricle by Masson staining. Scale bar: 1mm (left), 100um (right). B. Quantification of fibrosis in left ventricle. C. Quantification of left ventricular wall thickness. D. Representative images of cardiomyocytes in a remote area by HE staining. Scale bar: 50um. E. Quantification of cardiomyocyte cross-sectional area (CSA) in the remote area of the left ventricle. n=4-5/group, *P<0.05, **P<0.01, ***P<0.001.

Effects of BAK on gene expression levels in the infarcted and non-infarcted zones at seven days post-MI

The effect of BAK after MI on the expression of genes related to cardiac fibrosis and the myofibroblast differentiation, including TGF-β1, ERK1, ERK2, p38 MAPK, col1α1, col3α1, α-smooth muscle actin (SMA), and fibronectin was analyzed (Fig.3A-C). Gene expression of TGF-β1 and ERK2 increased after MI injury. Compared with the MI group, expression of TGF-β1 and ERK2 genes decreased significantly in the infarcted zone in the MI+BAK group; the presence of both genes in the non-infarcted zone showed a decreasing trend in the MI+BAK group. On the other hand, the expression of α-SMA and fibronectin genes increased after MI. BAK treatment did not significantly inhibit the expression of the α-SMA gene but inhibited fibronectin gene expression in the

infarcted and non-infarcted zones. ERK1, p38 MAPK, col1α1, and col3α1 did not improve after BAK treatment in the infarcted zone (Fig.3B).

Although improvements of cardiomyocyte hypertrophy in HE staining were not found, the effects of BAK treatment after MI on the expression of genes related to cardiac hypertrophy, including α-MHC, β-MHC, ANP, and BNP were analyzed (Fig.3A, C). The gene expression of β-MHC, ANP, and BNP increased, but α-MHC decreased in the infarcted and non-infarcted zones after MI. β-MHC and BNP gene expression were significantly reduced in the infarcted zone after BAK treatment, whereas the presence of α-MHC and ANP genes did not improve. α-MHC and ANP gene expression was greatly improved after BAK treatment in the non-infarcted zone, while β-MHC and BNP showed decreased trends.

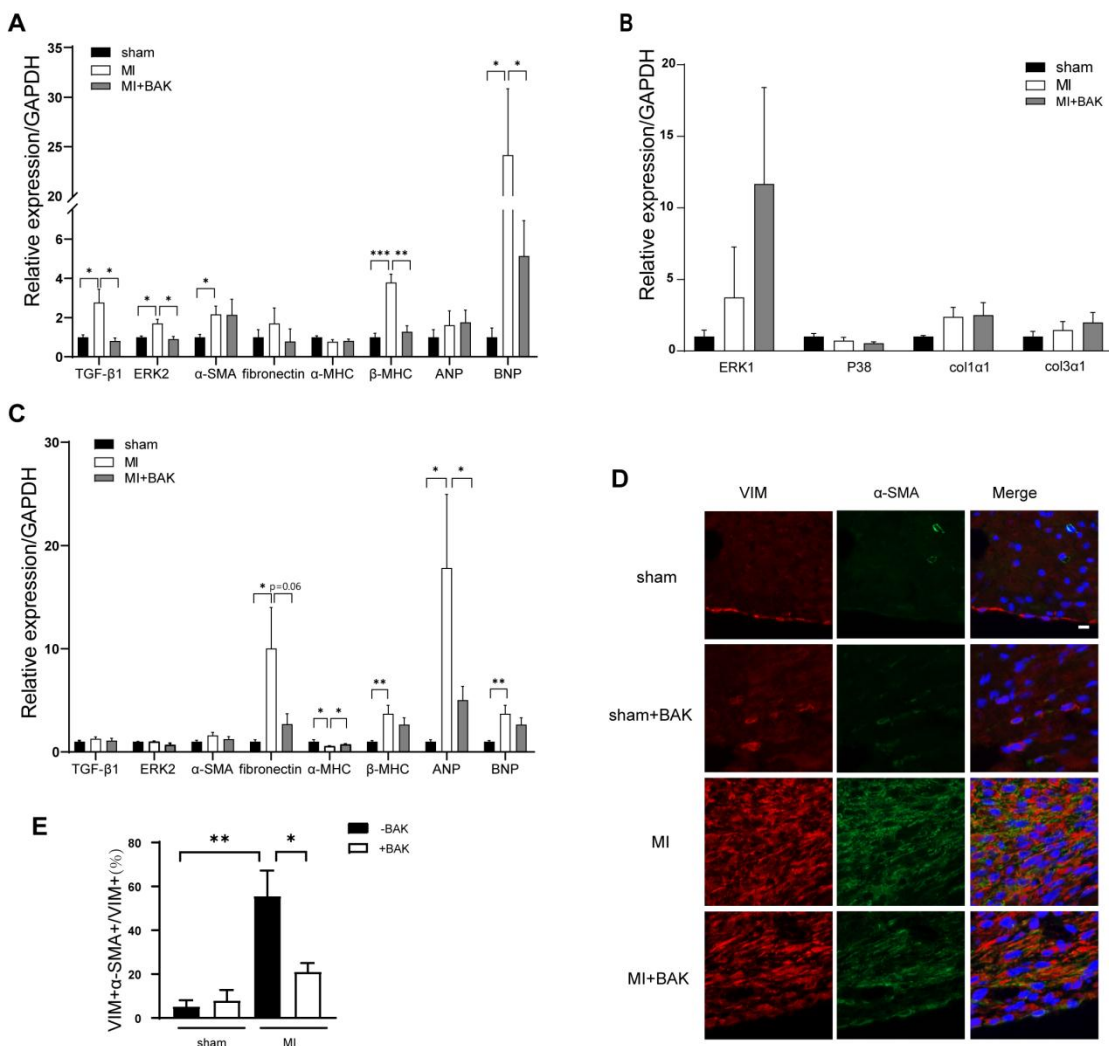


Fig.3. Effects of BAK on gene expression and cardiac myofibroblast differentiation in the heart at 7 days post MI. A and B. Gene expression in the infarcted zone. C. Gene expression in the non-infarcted zone. D.

Immunostaining for α -SMA and vimentin (VIM) in the scar at 7 days post MI. Scale bar: 10um. E. Qualification of the number of α -SMA expressing myofibroblasts. n=4-5/group, *P<0.05, **P<0.01, ***P<0.001.

Effects of BAK on cardiac myofibroblast differentiation at seven days post-MI

To explore the changes in cardiac myofibroblast differentiation after MI with BAK treatment, double immunofluorescence staining for α -SMA and vimentin (VIM, fibroblast marker) was performed. The number of myofibroblasts was defined as the fraction of the number of VIM+ α -SMA+ cells/ the number of VIM+cells, represents cardiac myofibroblast differentiation (28). Compared with the MI group, the level of myofibroblast differentiation was inhibited in the MI+BAK group (Fig.3D,E). Thus, BAK treatment can significantly inhibit cardiac myofibroblast differentiation at seven days post-MI.

Inhibition of ISO-induced cardiac fibroblast proliferation and migration by BAK

Without ISO stimulation, BAK (1, 2.5, and 5 μ M) did not affect cardiac fibroblast proliferation significantly

(Fig.4A). However, cardiac fibroblast proliferation had increased dramatically with ISO stimulation for 24 hours. BAK inhibited ISO-induced cardiac fibroblast proliferation in a dose-independent manner (Fig.4B). Transwell assays were used to verify the level of cardiac fibroblast migration (Fig.4C, D). The migration rate increased after ISO stimulation, but BAK treatment (1 μ M) inhibited the increase in ISO-induced migration rate (Fig.4D).

Effects of BAK on gene expression levels in cardiac fibroblasts stimulated with ISO

The expression of genes in ISO-stimulated cardiac fibroblasts with or without BAK was analyzed. Results showed that the gene expression of TGF- β 1, ERK2, α -SMA, and fibronectin significantly increased after ISO stimulation (Fig.4E). Conversely, BAK treatment inhibited the increase in expression of these genes in ISO-stimulated cardiac fibroblasts (Fig.4E).

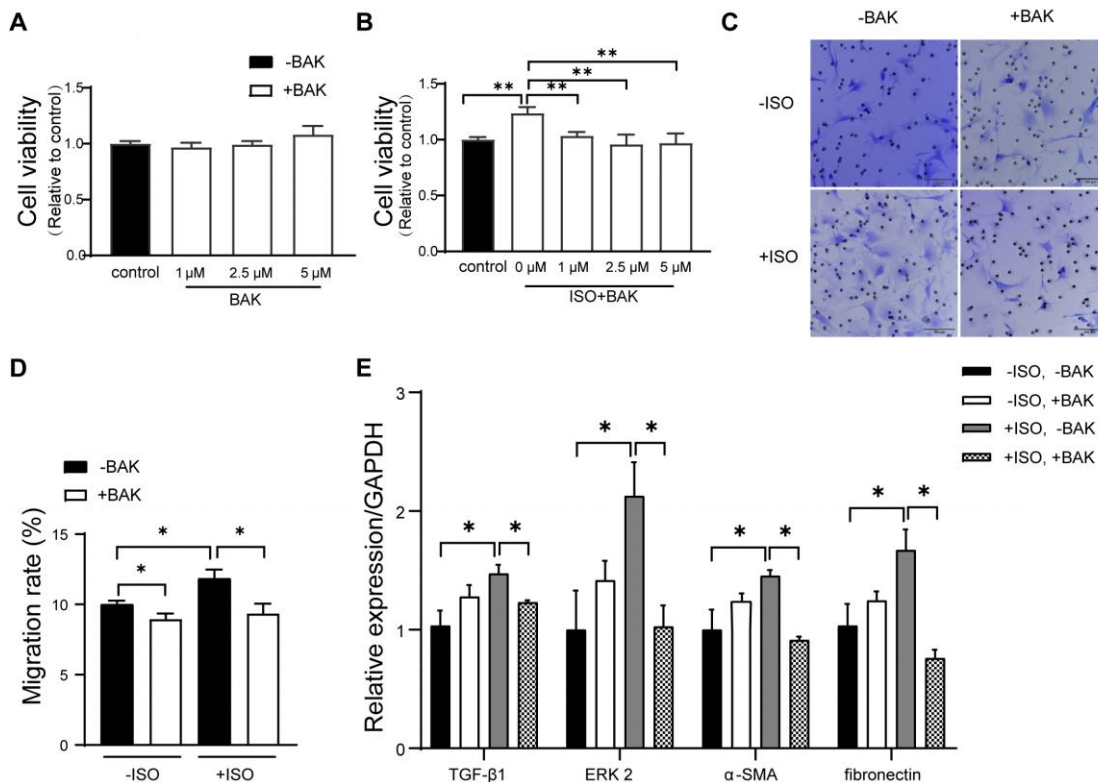


Fig.4. The effect of BAK on ISO-stimulated cardiac fibroblast. A and B. Cell proliferation detected by CCK-8. C. Representative images of the transwell assay; scale bar: 100 μ m. D. Quantification of migration rate. E. Gene expression in cardiac fibroblast. *P<0.05, **P<0.01, ***P<0.001.

Discussion

Following MI, progressive cardiac fibrosis reduces

myocardial compliance and function and leads to pathological cardiac remodeling (6). However,

effective treatments to improve cardiac function and prevent cardiac fibrosis are limited (6, 29). The present study demonstrated that BAK treatment significantly improved cardiac function and fibrosis after MI (Fig.1 and 2). In addition, BAK significantly inhibited cardiac fibroblast proliferation and migration, as well as myofibroblast differentiation (Fig.3 and 4). Thus, this study suggests that BAK may represent a novel therapeutic strategy for cardiac fibrosis after MI.

In the study, BAK treatment improved the LVEF at 7 and 28 days post-MI. And BAK has displayed protective effects on ischemia-reperfusion injury in the isolated heart (17), pressure overload-induced cardiac hypertrophy (18), and hyperglycemia-induced diabetic cardiomyopathy (19). Up until now, this study is the first to reveal the cardioprotective effects of BAK against MI injury. In previous studies, BAK treatment restrained deposition of collagen I and III to attenuate cardiac fibrosis in cardiac hypertrophy (18) and improved the cardiac function of diabetic myocardium (19). The two studies focused on the role of cardiomyocytes. However, in this study, the 28-day BAK treatment could not decrease the myocyte cross-sectional area in the heart. However, the treatment improved the expression of the genes related to cardiac hypertrophy, including α -MHC, β -MHC, ANP, and BNP at seven days. The treatment time may be insufficient in this study because BAK treatment for 12 weeks significantly improved hypertrophy in the previous study (19). As a result, we consider that the short-term BAK treatment in this research only improved the gene expression but did not change the cardiac structure.

This study focused more on the roles of BAK in cardiac function and cardiac fibrosis after MI. Cardiac fibroblasts, the central primary cells in the infarcted zone, are responsible for fibrosis (4) and scar formation after MI (30). Thus, this study aimed to determine if cardiac fibroblast migration, proliferation, and differentiation with BAK treatment, are closely related to cardiac fibrosis. Histologically, the results (Fig.2A-C) showed that BAK decreased cardiac fibrosis and increased ventricular wall thickness. Reducing cardiac fibrosis attenuates cardiac remodeling after MI (23). Furthermore, ventricular wall thickness is mechanical support to the integrity of the cardiac wall (6). Thus,

we considered that BAK could attenuate the influence of adverse remodeling on contraction after MI by lower fibrosis and wider ventricular wall thickness.

The results indicate that BAK treatment suppressed fibroblast proliferation and migration after ISO stimulation. The excessive proliferation and migration of the fibroblast can affect cardiac remodeling adversely (7,8). Restrained fibroblast proliferation improves scar organization and increases tensile strength to attenuate cardiac dysfunction and reduce dilative remodeling after MI (31). In this study, BAK treatment significantly inhibited fibronectin gene expression in vivo and vitro and α -SMA gene expression in vitro. Inhibiting fibronectin polymerization or gene expression in cardiac fibroblasts ameliorates cardiac remodeling and fibrosis (6).

Further, enhancement of gene expression of α -SMA and fibronectin is associated with myofibroblast differentiation (4,6,32). Meanwhile, immunofluorescence results showed that BAK treatment significantly decreased the number of myofibroblasts after myocardial infarction at seven days post-MI, which represents cardiac myofibroblast differentiation (28). The fibroblast differentiation at seven days is critical to the compensation of cardiac function compared to that at 28 days (8). In this study, BAK treatment also inhibits cardiac myofibroblast differentiation. Limiting myofibroblast differentiation and proliferation can attenuate post-infarction fibrosis and improve cardiac function (28, 33). Taken together, the data suggests that all these changes contributed to the prevention of adverse cardiac remodeling after MI.

The results demonstrated that BAK down regulated the gene expression of ERK2 and TGF- β 1 in the infarcted zone, where most dead cardiomyocytes were replaced by surrounding fibroblasts (7,8). But BAK did not improve the gene expression of other MAPKs. In addition, BAK increased the gene expression of ERK1 but decreased that of ERK2. BAK also downregulated the gene expression of ERK2 and TGF- β 1 in ISO-stimulated cardiac fibroblasts. TGF- β 1 and ERK2 are associated with regulating fibrosis in cardiac fibroblast (34). As the previous study demonstrated, inhibiting the ERK signaling pathway can

downregulate TGF- β 1 and α -SMA protein levels to attenuate renal interstitial fibrosis (35). TGF- β 1, which is released by cardiac fibroblasts or other cells in the injured heart (36), and is induced, and activated in the healing infarct scar which regulates myofibroblast differentiation (4, 31, 37). Therefore, this study hypothesized that BAK could have a protective effect on cardiac fibrosis and cardiac function by inhibiting the gene expression of ERK2 and TGF- β 1.

Conclusion: Cardiac fibrosis has been widely studied. However, the drugs that effectively inhibit myocardial fibrosis from improving cardiac function after MI are still scarce (4, 19, 31, 37). Therefore, this study demonstrates an exciting role of BAK in MI mice, which may be a potential therapeutic strategy for cardiac remodeling.

Funding

The grants of the present work were supported by the Natural Science Foundation of Shanghai (18ZR1432800), the Shanghai Municipal Commission of Health and Family Planning (201740176) and Health Committee of Jing'an District, Shanghai (2021QN01).

Conflicts of interest

All authors of this article have no conflicts of interest.

References

1. TALLQUIST M D, MOLKENTIN J D. Redefining the identity of cardiac fibroblasts[J]. *Nat Rev Cardiol*, 2017,14(8): 484-491.
2. FREY N, OLSON E N. Cardiac Hypertrophy: The Good, the Bad, and the Ugly[J]. *Annual Review of Physiology*, 2003,65(1): 45-79.
3. BERNARDO B C, WEEKS K L, PRETORIUS L, et al. Molecular distinction between physiological and pathological cardiac hypertrophy: Experimental findings and therapeutic strategies[J]. *Pharmacology & Therapeutics*, 2010,128(1): 191-227.
4. TALLQUIST M D. Cardiac Fibroblast Diversity[J]. *Annu Rev Physiol*, 2020,82: 63-78.
5. DOSTAL D, GLASER S, BAUDINO T A. Cardiac fibroblast physiology and pathology[J]. *Comprehensive Physiology*, 2015,5(2): 887.
6. VALIENTE-ALANDI I, POTTER S J, SALVADOR A M, et al. Inhibiting Fibronectin Attenuates Fibrosis and Improves Cardiac Function in a Model of Heart Failure[J]. *Circulation*, 2018,138(12): 1236-1252.
7. FU X, KHALIL H, KANISICAK O, et al. Specialized fibroblast differentiated states underlie scar formation in the infarcted mouse heart[J]. *Journal of Clinical Investigation*, 2018,128(5): 2127-2143.
8. ESCHENHAGEN T. A new concept of fibroblast dynamics in post-myocardial infarction remodeling[J]. *J Clin Invest*, 2018,128(5): 1731-1733.
9. CHOPRA B, DHINGRA A K, DHAR K L. *Psoralea corylifolia* L. (Buguchi) — Folklore to modern evidence: Review[J]. *Fitoterapia*, 2013,90: 44-56.
10. FERRÁNDIZ M L, GIL B, SANZ M J, et al. Effect of Bakuchiol on Leukocyte Functions and Some Inflammatory Responses in Mice[J]. *Journal of pharmacy and pharmacology*, 1996,48(9): 975-980.
11. CHOI S Y, LEE S, CHOI W, et al. Isolation and Anti-Inflammatory Activity of Bakuchiol from *Ulmus davidiana* var. *japonica*[J]. *Journal of Medicinal Food*, 2010,13(4): 1019-1023.
12. CHAUDHURI R K, BOJANOWSKI K. Bakuchiol: a retinol-like functional compound revealed by gene expression profiling and clinically proven to have anti-aging effects[J]. *Int J Cosmet Sci*, 2014,36(3): 221-230.
13. SEO E, OH Y S, KIM D, et al. Protective Role of *Psoralea corylifolia* L. Seed Extract against Hepatic Mitochondrial Dysfunction Induced by Oxidative Stress or Aging[J]. *Evidence-Based Complementary and Alternative Medicine*, 2013,2013: 1-9.
14. PARK E, ZHAO Y, KIM Y, et al. Bakuchiol-induced caspase-3-dependent apoptosis occurs through c-Jun NH2-terminal kinase-mediated mitochondrial translocation of Bax in rat liver myofibroblasts[J]. *European Journal of Pharmacology*, 2007,559(2-3): 115-123.
15. ZHANG X, CHANG N, ZHANG Y, et al. Bakuchiol Protects Against Acute Lung Injury

- in Septic Mice[J]. *Inflammation*, 2017,40(2): 351-359.
16. KIM K, SHIM S H, AHN H R, et al. Protective effects of the compounds isolated from the seed of *Psoralea corylifolia* on oxidative stress-induced retinal damage[J]. *Toxicology and Applied Pharmacology*, 2013,269(2): 109-120.
17. FENG J, YANG Y, ZHOU Y, et al. Bakuchiol attenuates myocardial ischemia reperfusion injury by maintaining mitochondrial function: the role of silent information regulator 1[J]. *Apoptosis*, 2016,21(5): 532-545.
18. WANG Z, GAO L, XIAO L, et al. Bakuchiol protects against pathological cardiac hypertrophy by blocking NF- κ B signaling pathway[J]. *Bioscience Reports*, 2018,38(5).
19. MA W, GUO W, SHANG F, et al. Bakuchiol Alleviates Hyperglycemia-Induced Diabetic Cardiomyopathy by Reducing Myocardial Oxidative Stress via Activating the SIRT1/Nrf2 Signaling Pathway[J]. *Oxidative Medicine and Cellular Longevity*, 2020,2020: 1-15.
20. MOLKENTIN J D, BUGG D, GHEARING N, et al. Fibroblast-Specific Genetic Manipulation of p38 Mitogen-Activated Protein Kinase In Vivo Reveals Its Central Regulatory Role in Fibrosis[J]. *Circulation*, 2017,136(6): 549-561.
21. MAO H, WANG H, MA S, et al. Bidirectional regulation of Bakuchiol, an estrogenic-like compound, on catecholamine secretion[M]. 2014: 180-189.
22. LI Z J, ABULIZI A, ZHAO G L, et al. Bakuchiol Contributes to the Hepatotoxicity of *Psoralea corylifolia* in Rats[J]. *Phytother Res*, 2017,31(8): 1265-1272.
23. CAMERON S J, TURE S K, MICKELSEN D, et al. Platelet Extracellular Regulated Protein Kinase 5 Is a Redox Switch and Triggers Maladaptive Platelet Responses and Myocardial Infarct Expansion[J]. *Circulation*, 2015,132(1): 47-58.
24. LI Y, WANG L, DONG Z, et al. Cardioprotection of salvianolic acid B and ginsenoside Rg1 combination on subacute myocardial infarction and the underlying mechanism[J]. *Phytomedicine*, 2019,57: 255-261.
25. ZHANG N, WEI W, LIAO H, et al. AdipoRon, an adiponectin receptor agonist, attenuates cardiac remodeling induced by pressure overload[J]. *Journal of Molecular Medicine*, 2018,96(12): 1345-1357.
26. CHE Y, SHEN D, WANG Z, et al. Protective role of berberine in isoprenaline-induced cardiac fibrosis in rats[J]. *BMC Cardiovascular Disorders*, 2019,19(1).
27. DAI H, JIA G, LU M, et al. Astragaloside IV inhibits isoprenaline-induced cardiac fibrosis by targeting the reactive oxygen species/mitogen-activated protein kinase signaling axis[J]. *Molecular Medicine Reports*, 2017,15(4): 1765-1770.
28. YOKOTA T, MCCOURT J, MA F, et al. Type V Collagen in Scar Tissue Regulates the Size of Scar after Heart Injury[J]. *Cell*, 2020,182(3): 545-562.
29. CHOTHANI S, SCHÄFER S, ADAMI E, et al. Widespread Translational Control of Fibrosis in the Human Heart by RNA-Binding Proteins[J]. *Circulation*, 2019.
30. FU X, KHALIL H, KANISICAK O, et al. Specialized fibroblast differentiated states underlie scar formation in the infarcted mouse heart[J]. *Journal of Clinical Investigation*, 2018,128(5): 2127-2143.
31. KONG P, SHINDE A V, SU Y, et al. Opposing Actions of Fibroblast and Cardiomyocyte Smad3 Signaling in the Infarcted Myocardium[J]. *Circulation*, 2018,137(7): 707-724.
32. COELHO L L, PEREIRA I R, PEREIRA M C D S, et al. *Trypanosoma cruzi* activates mouse cardiac fibroblasts in vitro leading to fibroblast-myofibroblast transition and increase in expression of extracellular matrix proteins[J]. *Parasites & Vectors*, 2018,11(1).
33. FRANCISCO J, ZHANG Y, JEONG J I, et al. Blockade of Fibroblast YAP Attenuates Cardiac Fibrosis and Dysfunction Through MRTF-A Inhibition[J]. *JACC: Basic to Translational Science*, 2020,5(9): 931-945.
34. LI L, FAN D, WANG C, et al. Angiotensin II increases periostin expression via Ras/p38 MAPK/CREB and ERK1/2/TGF- β 1 pathways

- in cardiac fibroblasts[J]. *Cardiovascular Research*, 2011,91(1): 80-89.
35. TANG C R, LUO S G, LIN X, et al. Silenced miR-21 inhibits renal interstitial fibrosis via targeting ERK1/2 signaling pathway in mice[J]. *Eur Rev Med Pharmacol Sci*, 2019,23(3 Suppl): 110-116.
36. RUWHOF C, van WAMEL A E, EGAS J M, et al. Cyclic stretch induces the release of growth promoting factors from cultured neonatal cardiomyocytes and cardiac fibroblasts[J]. *Mol Cell Biochem*, 2000,208(1-2): 89-98.
37. RODRIGUEZ P, SASSI Y, TRONCONE L, et al. Deletion of delta-like 1 homologue accelerates fibroblast–myofibroblast differentiation and induces myocardial fibrosis[J]. *European Heart Journal*, 2019,40(12): 967-978.